Journal of Nuclear Materials 384 (2009) 268–273

Contents lists available at ScienceDirect

Journal of Nuclear Materials

journal homepage: www.elsevier.com/locate/jnucmat

Characterization of the interaction layer grown by interdiffusion between U–7wt%Mo and Al A356 alloy at 550 and 340 °C

M. Mirandou [a,*], S. Aricó [a], M. Rosenbusch [b], M. Ortiz [a], S. Balart [a], L. Gribaudo [a,c]

[a] Departamento Materiales, GIDAT-GAEN-CNEA Av. Gral. Paz 1499, B1650KNA, San Martín, Argentina
[b] Departamento Química de Reactores, GIDAT-GAEN-CNEA Av. Gral. Paz 1499, B1650KNA, San Martín, Argentina
[c] Consejo Nacional de Investigaciones Científicas y Tecnológicas Avda. Rivadavia 1917, C1033AAJ, Buenos Aires, Argentina

ARTICLE INFO

Article history:
Received 10 March 2008
Accepted 25 November 2008

PACS:
28.50.Dr
61.10.Nz
66.30.Ny

ABSTRACT

U(Mo) alloys are under study to get a low-enriched U fuel for research and test reactors. Qualification experiments of dispersion fuel elements have shown that the interaction layer between the U(Mo) particles and the Al matrix behaves unsatisfactorily. The addition of Si to Al seems to be a good solution. The goal of this work is to identify the phases constituting the interaction layer for out-of-pile interdiffusion couples U(Mo)/Al(Si). Samples γU–7wt%Mo/Al A356 alloy (7.1 wt%Si) made by Friction Stir Welding were annealed at 550 and 340 °C. Results from metallography, microanalysis and X-ray diffraction, indicate that the interaction layer at 550 °C is formed by the phases $U(Al,Si)_3$, U_3Si_5 and $Al_{20}Mo_2U$, while at 340 °C it is formed by $U(Al,Si)_3$ and U_3Si_5. X-ray diffraction with synchrotron radiation showed that the Si-rich phase, previously reported in the interaction layer at 550 °C near U(Mo) alloy, is U_3Si_5.

1. Introduction

The use of dispersion or monolithic fuel elements containing low-enriched uranium (LEU) γU(Mo) alloys as fuel in the conversion of high flux research nuclear reactors is under study [1]. Pos irradiation experiments (PIE) have shown a significant interaction layer (IL) grown by interdiffusion between γU(Mo) alloy and the Al matrix producing a considerable swelling and, in some cases, an unacceptable porosity located in the interface between the IL and the Al [2–5]. This porosity is related to a poor irradiation behavior of the phases that form this IL [3,6].

Out-of-pile research works on diffusion couples γU(5 wt%Mo, 7 wt%Mo, 10 wt%Mo)/Al between 500 and 600 °C have been reported. The study of the IL made by composition determinations [7–9] and also by crystalline structure identification using X-ray diffraction (XRD) [10] has indicated that this is a multibanded zone formed by UAl_3, UAl_4 and $Al_{20}Mo_2U$ type phases. Micro-X-ray absorption spectroscopy (μ-XAS) tests [11] indicated that the solubility of Mo in UAl_3 and UAl_4 is very low and micro-X-ray diffraction mapping (μ-XRD) tests [11] showed that at least one ternary UMo_yAl_x phase can be identified at each probed area in the IL.

One way to mitigate swelling is to modify the composition of the IL. In Ref. [3], on the basis of previous literature and data from fuel manufacturing [12–14], it was proposed to change the matrix by adding Si to Al. These works reported that this change in the U/Al system resulted in the suppression of the intermetallic UAl_4, the migration of Si towards the IL and the reduction of the IL growth rate. The first results in out-of-pile interdiffusion experiments performed in this laboratory confirmed that the first two effects derived from Si, mentioned above, are also observed in a diffusion couple U–7wt%Mo/Al A356 alloy (7.1 wt%Si) and Al 4043 alloy (5.2 wt%Si) at 550 °C [15]. Subsequent investigations concerning the addition of Si to Al matrix were also reported [16–21] and they all show accumulation of Si in the IL and thickness reduction compared to diffusion couples between γU(Mo) and pure Al. In Ref. [21] it was shown that the simultaneous presence of Si in the Al and Zr in the γU(Mo) enhances this effect.

This change in the matrix of dispersion fuel elements is currently being tested under irradiation with positive results [22,23].

This work presents results of out-of-pile interdiffusion experiments in couples γU–7wt%Mo/Al A356 alloy (7.1 wt%Si) at 550 and 340 °C and focuses on the identification of the crystalline structure of the phases that form the IL. XRD performed with conventional diffractometer and with synchrotron radiation (Brazilian Synchrotron Light Laboratory (LNLS), Campinas, Brazil) are used to identify the phases together with optical microscopy observations and composition determination analysis.

2. Experimental

The U–7wt%Mo alloy was made by arc melting in a small non-consumable tungsten electrode arc-furnace with a copper crucible under highly pure argon atmosphere. Depleted U (0.2 at.% ^{235}U

* Corresponding author. Tel.: +54 11 6772 7222; fax: +54 11 6772 7362.
E-mail address: mirandou@cnea.gov.ar (M. Mirandou).

0022-3115/$ - see front matter © 2009 Published by Elsevier B.V.
doi:10.1016/j.jnucmat.2008.11.035

with principal impurities: 27 wppm Fe, 60 wppm Mg, 24 wppm Si and <10 wppm Al) and Mo 99.97 wt% (<20 wppm O_2, <10 wppm N_2, <10 wppm C, <100 wppm W, 8 wppm Si and 2 wppm Ni) were used. Specimens, in the as-cast condition, were homogenized in composition by a heat treatment of 2 h at 1000 °C, under argon atmosphere, using quartz tubes. Water quenching without tube breaking was used to retain γU(Mo) in metastable condition.

The commercial Al A356 alloy (nominal composition: 7.1 wt%Si, 0.37 wt%Mg, 0.12 wt%Ti, 0.10 wt%Fe, 0.02 wt%Zn, 0.01 wt%Ca, 0.001 wt%Sr) was used as provided by the manufacturer. In this condition, most of the Si present in the Al alloy forms pure needle-shaped Si precipitates located in the Al grain boundaries.

Diffusion couples were made by friction stir welding technique (FSW) [24]. Pieces of $(15 \times 5 \times 0.5)\,mm^3$ were cut from U–7wt%Mo alloy. Parallel faces and rounded corners were obtained by mechanical polishing up to 1 μm diamond paste. Plates of $(50 \times 70 \times 2)\,mm^3$ and $(50 \times 70 \times 2.5)\,mm^3$ were cut from Al A356 ingot and machined with parallel faces to be used as lid and base, respectively. They were degreased before used.

Each U–7wt%Mo piece was placed in a cavity machined on the Al A356 base plate and covered with the lid. The whole set was kept tight. In the FSW process, a cylindrical rotating tool is impinged on the lid and as the tool is moved along the length of the Al alloy, produces the plastification of the Al alloy and dispersion of possible oxide layers. When the rotating tool passes close enough over the U(Mo) foil, smears the Al alloy onto its surface giving a good interfacial contact. The set is machined flat, turned upside down and the operation repeated. As result of this process, U(Mo) foil is surrounded by Al A356 and has no contact with air. As a consequence of FSW, needle-shaped Si precipitates, as mentioned above, turned into round ones and homogenously distributed.

Thermal treatments were performed in an electric resistance tubular alumina furnace. As U–7wt%Mo alloy is embedded in Al A356, no protecting atmosphere was used. After each thermal treatment the diffusion couples were quenched in cold water. Diffusion anneals were performed from 1.5 h to 3.6 h at 550 °C (samples ***I*** and ***II***) and from 552 h to 2640 h at 340 °C (samples ***III*** and ***IV***), Table 1. At both temperatures, successive thermal treatments were performed in order to enlarge the thickness of the IL. At high temperature, lengths of the anneals were selected trying to avoid γU(Mo) phase decomposition with cellular lamellar morphology [25,26]. In spite of this, decomposition was observed in some cases.

The characterization of ILs was performed by optical microscopy (OM – Olympus BX60M), scanning electron microscopy (SEM – Philips SEM 515), energy dispersive spectroscopy (EDS – EDAX Phoenix 3.2), wavelength dispersive spectroscopy (WDS – CAMECA SX50) and X-ray diffraction with a conventional diffractometer (XRD – Philips PW3710) or with synchrotron radiation (XRD – Line XRD1, Brazilian Synchrotron Light Laboratory).

Table 1
Details of the diffusion anneals, thicknesses of ILs and precipitate free zones (PFZs).

Sample	Diffusion anneals		IL (μm)	PFZ (μm)
	T (°C)	Time (h)		
I	550	1.5	9	55
		1.5 + 1.5	13	79
		1.5 + 1.5 + 0.6	14	83
II		1.5	10	46
		1.5 + 1.5	12	61
III	340	624	5	33
		624 + 432	7	55
		624 + 432 + 1008	11	78
IV		552	–	–
		552 + 2088	13	100

The quantitative compositional microanalysis by WDS was made under an accelerating potential of 20 kV. The equipment was recalibrated before each analysis session using pure 99.99 wt%U, 99.99 wt%Mo, 99.99 wt%Al and 99.999 wt%Si standards.

XRD measurements with conventional diffractometer were performed with filtered Cu $K\alpha$ radiation, $\lambda = 0.1540$ nm, at room temperature. When synchrotron radiation was used, an energy of 8.014 keV was selected resulting in $\lambda = 0.1547$ nm obtained by the use of the LaB_6 diffraction pattern. For both cases, powder diffraction technique was applied to bulk samples. Crystalline structure identification and the estimation of the lattice parameters were obtained by the use of PowderCell program [27].

Samples used to study the IL by OM, SEM, EDS and WDS were cut perpendicular to the diffusion front in order to expose the whole IL simultaneously. They were grinded and mechanically polished up to 1 μm diamond paste followed by chemical etching (1% v/v HF) before characterization. Samples used for characterization by XRD were polished at a small angle to the diffusion front in order to enlarge the intersection between the IL and the exposed area. In this case, they were grinded and mechanically polished up to 1 μm diamond paste before the diffraction experiments.

3. Results

Common features found for both temperatures were as follows: after the first diffusion anneal, an IL was observed between the U(Mo) and the Al A356 for all the samples, a precipitate free zone (PFZ) appeared due to the dissolution of Si precipitates in the Al alloy and successive thermal treatments resulted in enlarged IL and PFZ.

3.1. Interdiffusion at 550 °C

All the ILs showed planar interfaces and almost constant widths. The PFZs were wider than its associated IL, Fig. 1. An enlargement in the IL was always accompanied by an enlargement in its corresponding PFZ, Table 1.

Values reported in Table 1 for IL and PFZ result from the average of 10 measurements taken in different places with an eye-piece micrometer (appreciation ± 1 μm). The standard deviations were about 10% for each IL and 5% for each PFZ.

For both samples after each thermal treatment, two different zones could be identified inside the ILs. Both zones are labeled as *Zone 1*, near U–Mo, and *Zone 2*, near Al A356 and are separated by a dot line in Fig. 2. *Zone 1* showed a banded morphology and an important longitudinal crack.

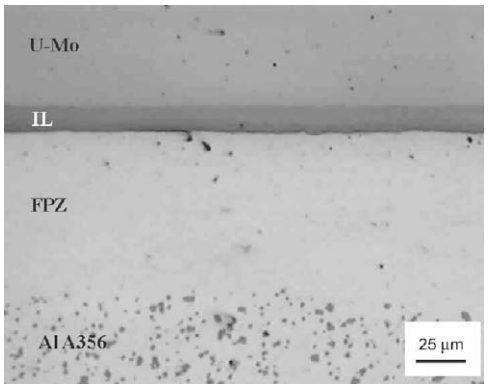

Fig. 1. Sample ***I***. 550 °C–(1.5 + 1.5 + 0.6) h. IL with planar interfaces and the associated PFZ. Si precipitates in gray in Al A356. OM, mechanical polishing.

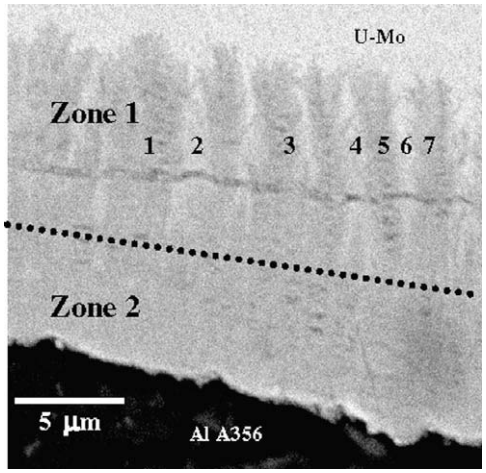

Fig. 2. Sample ***II***. 550 °C–(1.5 + 1.5) h. IL (*Zone 1* + *Zone 2*) morphology. Numbers 1 to 7 indicate the place of composition determinations in *Zone 1*. SEM, mechanical polishing.

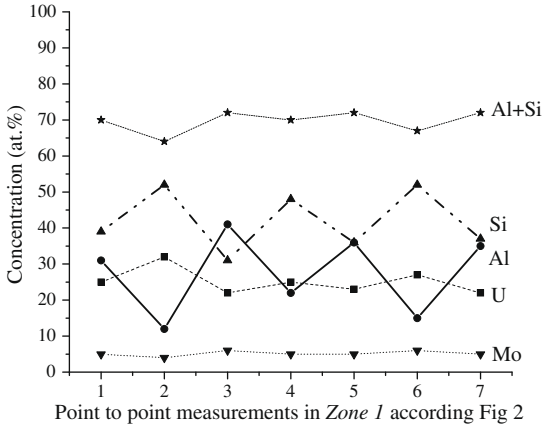

Fig. 3. Sample ***II***. 550 °C–(1.5 + 1.5) h. Values of composition determinations performed in *Zone 1*. EDS.

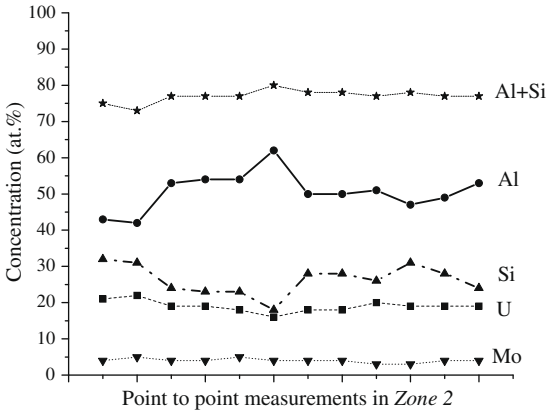

Fig. 4. Sample ***II***. 550 °C–(1.5 + 1.5) h. Values of composition determinations performed in *Zone 2*. EDS.

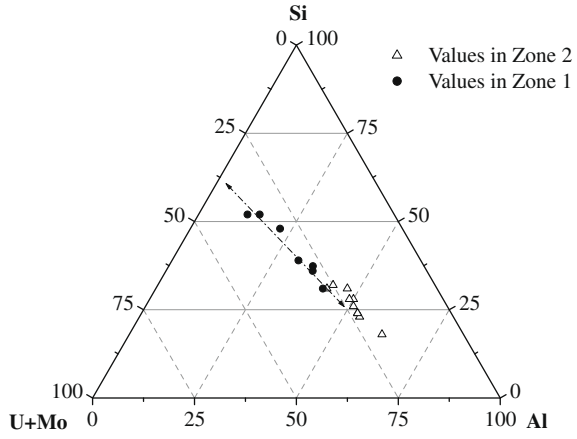

Fig. 5. Sample ***II***. 550 °C–(1.5 + 1.5) h. Values of composition determinations in at.%. Pseudo ternary representation (U + Mo)-Al–Si. EDS.

Point to point composition determinations by EDS were performed on both zones. In *Zone 1*, due to the narrowness of the bands, each measurement corresponds to a different proportion of both bands. Nevertheless, in a small region of sample ***II*** (1.5 h + 1.5 h), in which these bands were found to be slightly wider, an attempt to find differences in composition between the bands was made. Results for U, Mo, Al and Si are plotted in Fig. 3. Significant differences in the amount of Si and Al were found between points 1, 3, 5 and 7 (Fig. 2, dark bands) and points 2, 4 and 6 (Fig. 2, light bands). In these last bands, Si content reached its highest value (around 50 at.%). The addition Al + Si is also included in Fig. 3. As it is shown, this sum remains almost constant around 72 at.% for the dark bands while lower values were obtained for light bands. Composition determinations in *Zone 2* were performed randomly along the whole IL. Values plotted in Fig. 4 show that Si content is always lower than the Al content and fluctuates around 25 at.% while Al does it around 50 at.%. Although both elements present significant fluctuations around its average values, their addition remains almost constant at about 75 at.%.

These composition determinations performed in *Zone 1* and *2* in sample ***II*** are plotted in a pseudo ternary representation (U + Mo)–Al–Si in Fig. 5. This representation was considered appropriate because the ratio U/Mo measured in the IL remains as in the original U–7wt%Mo alloy. Measurements from *Zone 2* accumulate around (U + Mo)–50 at.%Al–25 at.%Si, while measurements from *Zone 1* spread on a line whose ends point to the compositions (U + Mo)–50 at.%Al–25 at.%Si and (U + Mo)–62.5 at.%Si. Similar behavior of the composition determinations was also observed for the thermal treatments on sample ***I***.

XRD with conventional diffractometer showed γU phase and αU phase from the U(Mo) alloy, Al phase and typical precipitates from Al A356 alloy and only $U(Al,Si)_3$ compound with lattice parameter $a \sim 0.418$ nm from the IL. This lattice parameter value can be associated to a concentration of about 36 at.%Si, in this compound, according to the correlation between lattice parameter and Si concentration presented in Fig. 19 in Ref. [28].

Because previous techniques suggest the existence of more than one phase inside the IL, XRD characterization was improved by using synchrotron radiation. Three crystalline structures corresponding to the phases that form the IL were identified: $U(Al,Si)_3$ with lattice parameter $a \sim 0.419$ nm (35 at.%Si according to Fig. 19 in Ref. [28]), the ternary compound $Al_{20}Mo_2U$ and the hexagonal hP3, AlB_2 *type*, U_3Si_5 [28] with lattice parameters $a \sim 0.392$ nm and $c \sim 0.405$ nm, Fig. 6.

3.2. Interdiffusion at 340 °C

All the ILs showed planar interfaces but not uniform widths. Widened zones were found in both samples and taken into account, proportionally, to estimate width in Table 1. Accordingly, standard deviations were about 30%. Each IL was again accompa-

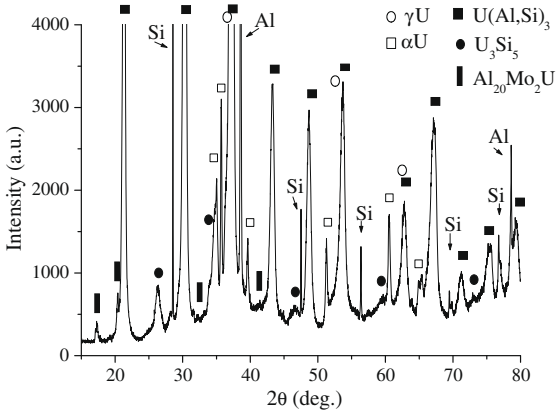

Fig. 6. Sample ***II***. 550 °C–(1.5 + 1.5) h. Phase identification in the diffusion couple. Full symbols correspond to phases in the IL. XRD with synchrotron radiation.

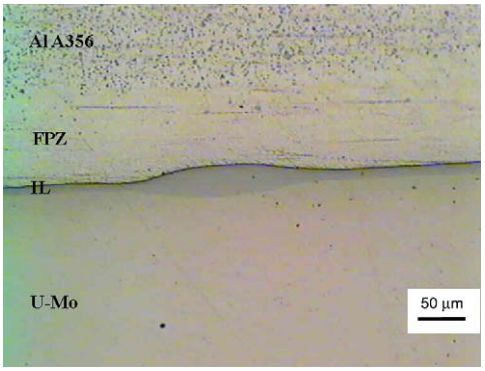

Fig. 7. Sample ***IV***. 340 °C–(552 + 2088) h. IL with planar interfaces and the associated PFZ. Si precipitates in gray in Al A356. OM, mechanical polishing.

nied by a PFZ, Fig. 7, with a standard deviation, on the width, of about 10%. At this temperature the ratio PFZ/IL was higher than the corresponding one at 550 °C.

On sample ***III***, after each diffusion anneal, 5–10 point to point measurements were done along the whole IL and plotted in a pseudo ternary representation (U + Mo)–Al–Si, Fig. 8. No spread in composition was observed from each annealing stage. A slight Al increment is suggested when comparing the three stages.

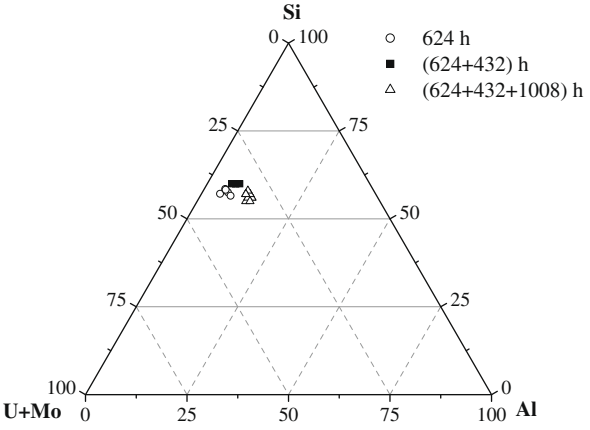

Fig. 8. Sample ***III***. 340 °C. Values of composition determinations in at.%. Pseudo ternary representation (U + Mo)-Al-Si. (■) and (○) by WDS and (△) by EDS.

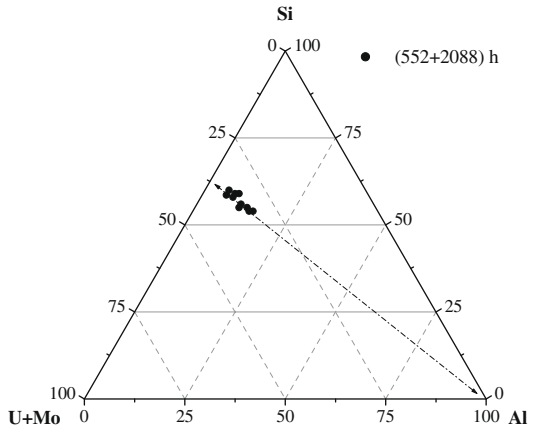

Fig. 9. Sample ***IV***. 340 °C–(552 + 2088) h. Values of composition determinations in at.%. Pseudo ternary representation (U + Mo)–Al–Si. EDS.

On sample ***IV*** 10 point to point measurements were done after the second diffusion anneal and are shown in Fig. 9. In this case, composition values spread on a line whose ends point to the compositions (U + Mo)–62.5 at.%Si and pure Al.

XRD was performed on sample ***IV*** with conventional diffractometer after the first diffusion anneal and with synchrotron radiation after the second one. Crystalline structures corresponding to γU and αU from the U(Mo) alloy and Al and/or typical precipitates from Al A356 alloy were identified from both diffusion anneals. Concerning the IL, U_3Si_5 with lattice parameters $a \sim 0.397$ nm and $c \sim 0.403$ nm together with $U(Al,Si)_3$ with lattice parameter $a \sim 0.416$ nm were identified, Figs. 10(a) and (b). According to Fig. 19 in Ref. [28], the lattice parameter value estimated for $U(Al,Si)_3$ can be associated to ~42 at.%Si. Comparing both spectra, the one obtained with conventional diffractometer allowed a better estimation of $U(Al,Si)_3$ lattice parameter while the obtained with synchrotron radiation proved to be better to estimate U_3Si_5 lattice parameters.

4. Discussion

In this work, the interaction layer grown by interdiffusion between U–7 wt%Mo and Al A356 (7.1 wt%Si) was studied on samples annealed at two temperatures, 550 and 340 °C.

The dissolution of pure Si precipitates, creating the PFZ in the Al A356 alloy, and the displacement of Si atoms towards the IL, are the cause of the significant amount of Si found inside it at both

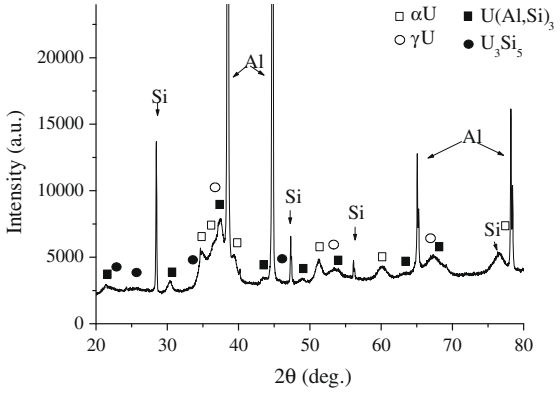

Fig. 10a. Sample ***IV***. 340 °C–552 h. Phase identification in the diffusion couple. Full symbols correspond to phases in the IL. XRD with conventional diffractometer.

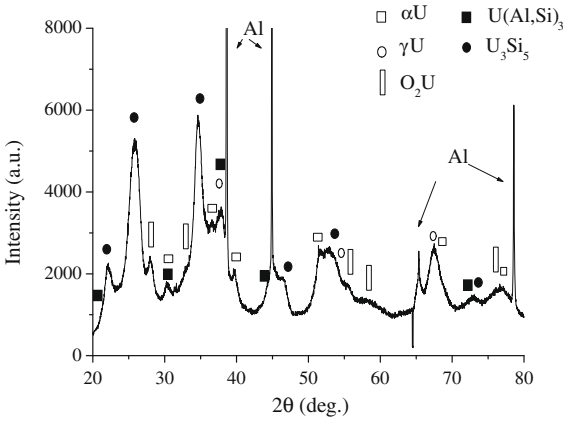

Fig. 10b. Sample ***IV***. 340 °C–(552 + 2088) h. Phase identification in the diffusion couple. Full symbols correspond to phases in the IL. XRD with synchrotron radiation.

temperatures. This Si accumulation was also observed by [15,18,21] in similar experiments. Taking into account the IL and PFZ widths presented in Table 1, the ratio PFZ/IL resulted larger at 340 °C than at 550 °C. This is associated to the higher Si content measured in the IL at 340 °C, Figs. 8 and 9, than at 550 °C, Fig. 5.

At 550 °C, considering the information gathered with all the characterization techniques, the phases in the IL were: $U(Al,Si)_3$, U_3Si_5 and $Al_{20}Mo_2U$. Composition measurements plotted in Fig. 5 suggest that the phases $U(Al,Si)_3$ and U_3Si_5 are associated to the banded morphology in *Zone 1* while only $U(Al,Si)_3$ is associated to *Zone 2*. The $Al_{20}Mo_2U$ phase could be assigned to any zone inside the IL because its spatial location could not be confirmed.

At 340 °C, considering the information gathered with all the techniques, $U(Al,Si)_3$ and U_3Si_5 are the phases that form the IL, having no specific location inside it. $Al_{20}Mo_2U$ was not identified at this temperature.

Comparing the estimated lattice parameter for the phase $U(Al,Si)_3$ identified by XRD at both temperatures, the decrease in its value obtained at 340 °C ($a \sim 0.416$ nm) with respect to the value obtained at 550 °C ($a \sim 0.419$ nm) is known to be associated to an increment in Si concentration present in this phase [28]. The Si concentration in $U(Al,Si)_3$ was obtained by two different methods: direct measurement (EDS or WDS) and estimation from the lattice parameter obtained from XRD patterns using Dwight correlation (Fig. 19 in Ref. [28]). When comparing results from both methods at 550 °C (25 at.% Si and 35 at.% Si, respectively) it was observed that the agreement is not satisfactory. In this sense, it is important to take into account that $Al_{20}Mo_2U$ phase could not be spatially located inside the IL and, if a fine dispersion is supposed, it could affect the interpretation of composition measurements. Based on this explanation, the 35 at.%Si, indirectly obtained from XRD, is adopted. When comparing both Si concentration results in $U(Al,Si)_3$ phase at 340 °C (44 at.%Si and 42 at.%Si), for which $Al_{20}Mo_2U$ phase was not identified, both methods showed a good agreement. The concentration of 44 at.%Si was obtained from the intersection between the dotted line and the 25 at.%(U + Mo) isopleth in Fig. 9.

Concerning U_3Si_5 phase, lattice parameters reported in this work were $a \sim 0.392$ nm and $c \sim 0.405$ nm at 550 °C and $a \sim 0.397$ nm and $c \sim 0.403$ nm at 340 °C while the original lattice parameters reported for this phase are $a = 0.3896$ nm and $c = 0.4017$ nm [28]. As it can be seen, an increment in the unit cell volume, with respect to the original one, was obtained in this work for both temperatures. According to Dwight [28], the crystalline structure of this phase is a defect type and a ternary element (e.g. Al) could either enter an empty lattice site or displace Si atom. In the isothermal section at 400 °C presented in Ref. [28], up to ~5 at.%Al is accepted by this phase. Nevertheless, no information of correlation between lattice parameters and the Al concentration could be found in literature. Composition measurements performed at both temperatures in this work (Figs. 5 and 9) suggest the presence of Al in this phase which could explain the cell volume increment mentioned above.

Previous out-of-pile diffusion investigations between U–Mo alloys and Al–Si alloys [15,21,29], found a high Si content inside the IL and agreed in the presence of a Si-rich phase near the U(Mo) alloy. In these works, proposed Si-rich phases were: $U(Si,Al)_{2-x}$, $U(Si,Al)_2$ and USi_2 type phase with Si accepting a few substitutions with Al and Mo, respectively. Nevertheless, according to the isothermal section at 400 °C in the U–Al–Si system presented in Ref. [28], there are four phases which existence domains would explain composition measurements showed in [15,21,29]: the binary compounds USi_{2-x}, USi_2, U_3Si_5 and the ternary intermetallic $Al_2Si_3U_3$. In this sense, it is evident that composition measurements alone are not enough to determine which of these four phases is, or are, present in the IL. XRD with synchrotron radiation experiments, presented in this work, showed that the Si-rich phase is the compound U_3Si_5.

It is important to remark that the phase UAl_4 was not found in the IL at 550 °C, as it was in diffusion couples U–Mo/Al at temperatures from 500 °C to 600 °C [7,8,10,11]. The effect of Si suppressing the formation of this phase at high temperature has already been reported by [12–14] for pure U. In this work, same effect is shown for U–7 wt%Mo alloy.

The results presented in this work are considered promising since a change in IL composition, with respect to the one with pure Al, has been obtained. Besides, $U(Al,Si)_3$ has been reported to be the interaction product in out-of-pile diffusion experiments between U_3Si and Al [30], and in PIE of U_3Si_2 dispersion fuel elements [31]. These fuel elements have shown a good performance under irradiation in normal conditions [31].

5. Conclusions

A complete characterization of the interaction layer grown by interdiffusion between U–7 wt%Mo and Al A356 alloy at 550 and 340 °C was achieved.

The dissolution of Si precipitates in the Al A356, creating the precipitate free zone, and the migration of this element are the causes of the accumulation of Si in the interaction layer.

The interaction layer at 550 °C is formed by the phases $U(Al,Si)_3$, U_3Si_5 and $Al_{20}Mo_2U$ while at 340 °C is formed by $U(Al,Si)_3$ and U_3Si_5.

XRD with synchrotron radiation experiments allowed going further in the phase identification at 340 °C and showed that the Si-rich phase, already reported in literature at 550 °C, is the hexagonal hP3, AlB_2 *type*, U_3Si_5 compound.

It was confirmed that the concentration of Si present in the Al A356 alloy avoids the formation of UAl_4 phase at 550 °C.

Acknowledgements

The authors want to thank Dr G. Hofman (ANL) for suggesting this investigation, the technical staff of Dto. Materiales (GIDAT, GAEN, CNEA) for their support, Pedro Cabot and Alberto Moglioni of ENDE (GIDAT, GAEN, CNEA) for the manufacture of the samples by FSW technique and Roosevelt Droppa Jr. from LNLS staff for training in synchrotron radiation equipment. This work was partially financed by Project PICT 12-11186, Agencia de Promoción Cientifica y Tecnológica (Argentina), Grant PIP 5062 CONICET

(Argentina) and Project D12A-XRD1·# 5747/06, LNLS, Campinas (Brazil).

References

[1] M.K. Meyer, G.L. Hofman, S.L. Hayes, C.R. Clark, T.C. Wiencek, J.L. Snelgrove, R.V. Starin, K.H. Kim, J. Nucl. Mater. 304 (2002) 221.
[2] A. Leenaers, S. Van den Berghe, E. Koonen, C. Jarousse, F. Huet, M. Trotabas, S. Boyard, M. Verwerft, J. Nucl. Mater. 335 (2004) 39.
[3] G.L. Hofman, M.R. Finlay, Y.S. Kim, in: Proceedings of the XXVI RERTR International Meeting, 7–12 November, 2004, Vienna, Austria.
[4] D.F. Sears, K.T. Conlon, J. Manson, A. Davidson, C. Buchnan, Transaction 10th International Topical Meeting ENS RRFM, 30 April–3 May 2006, Sofia, Bulgaria.
[5] V. Popov, V. Khmelevsky, A. Lukichev, O. Golosov, Transaction Ninth International Topical Meeting ENS RRFM, 10–13 April 2005, Budapest, Hungary.
[6] S. Van den Berghe, W. Van Renterghem, A. Leenaers, in: Proceedings of the XXIX RERTR International Meeting, 23–27th September 2007, Prague, Czech Republic.
[7] H.J. Ryu, Y.S. Han, J.M. Park, S.D. Park, C.K. Kim, J. Nucl. Mater. 321 (2003) 210.
[8] F. Mazaudier, C. Proye, F. Hodaj, Transaction 10th International Topical Meeting ENS RRFM, 30 April–3 May 2006, Sofia, Bulgaria.
[9] E. Perez, N. Hotaling, A. Ewh, D.D. Keiser, Y.H. Sohn, Defect and Diffusion 266 (2007) 149.
[10] M. Mirandou, S. Balart, M. Ortiz, M. Granovsky, J. Nucl. Mater. 323 (2003) 29.
[11] H. Palancher, P. Martin, V. Nassif, R. Tucoulou, O. Proux, J.L. Hazemann, O. Tougait, E. Lahéra, F. Mazaudier, C. Valot, S. Dubois, J. Appl. Crystallogr. 40 (2007) 1064.
[12] R. Boucher, J. Nucl. Mater. 1 (1959) 13.
[13] D.R. Green, HW 49697, April 1957.
[14] W.C. De Luca, H.T. Sumsion, KALP-1747 (1957).
[15] M. Mirandou, M. Granovsky, M. Ortiz, S. Balart, S. Aricó, L. Gribaudo, in: Proceedings of the XXVI RERTR International Meeting, 7–12 November 2004, Vienna, Austria.
[16] M. Mirandou, S. Aricó, L. Gribaudo, S. Balart, in: Proceedings of the XXVII RERTR International Meeting, 6–11 November 2005, Boston, Massachusetts, USA.
[17] C. Komar Varela, M. Mirandou, S. Aricó, S. Balart, L. Gribaudo, Eleventh International Topical Meeting ENS RRFM-IGORR, 11–15th March 2007, Lyon, France.
[18] M. Cornen, F. Mazaudier, X. Iltis, M. Rodier, S. Dubois, P. Lemoine, Eleventh International Topical Meeting ENS RRFM-IGORR, 11–15th March 2007, Lyon, France.
[19] C. Komar Varela, M. Mirandou, S. Aricó, S. Balart, L. Gribaudo, in: Proceedings of the XXIX RERTR International Meeting, 23–27th September 2007, Prague, Czech Republic.
[20] D. Keiser Jr., Defect and Difusión Forum, 266 (2007) 131.
[21] J.M. Park, H.J. Ryu, S.J. Oh, D.B. Lee, C.K. Kim, Y.S. Kim, G.L. Hofman, J. Nucl. Mater. 374 (3) (2008) 422.
[22] S. Dubois, J. Noirot, J.M. Gatt, M. Ripert, Eleventh International Topical Meeting ENS RRFM-IGORR, 11–15 March 2007, Lyon, France.
[23] G.L. Hofman, Y.S. Kim, H.J. Ryu, M.R. Finlay, Eleventh International Topical Meeting ENS RRFM-IGORR, 11–15 March 2007, Lyon, France.
[24] P. Cabot, A. Moglioni, M. Mirandou, S. Balart, in: Proceedings of the XXVI RERTR International Meeting, 7–12th November 2004, Vienna, Austria.
[25] D. Blake, R. Hehemann, Transformation in Uranium Base Alloys, in: J. Burke, D. Colling, A. Gorum, J. Greenspan (Eds.), Physical Metallurgy of Uranium Alloys, Brook Hill Publishing Co, Chestnut Hill, Massachusetts, 1976, pp. 189–218.
[26] C.L. Komar Varela, S.F. Aricó, L.M. Gribaudo, Actas del congreso SAM-CONAMET 2007, in press.
[27] W. Kraus, G. Nolze, U. Müller, PowderCell 2.3. – Pulverdiffraktogramme aus Einkristalldaten und Anpassung experimenteller Beugungsaufnahmen, 2000, <http://www.bam.de/de/service/publikationen/powder_cell_a.htm> .
[28] A.E. Dwight, Report Specification N° ANL-82-14 (1982) 1–39.
[29] M. Cornen, M. Rodier, X. Iltis, S. Dubois, P. Lemoine, Twelfth International Topical Meeting ENS RRFM, 3–5 March 2008, Hamburg, Germany.
[30] C-K. Rhee, S-I. Pyun, I-H. Kuk, J. Nucl. Mater. 184 (1991) 161.
[31] A. Leenaers, S. Van den Berghe, E. Koonen, P. Jacquet, C. Jarousse, B. Guigon, A. Ballagny, L. Sannen, J. Nucl. Mater. 327 (2004) 121.